

# A Novel Approach To Sogi Grid Synchronization System For Three-Phase Grid-Connected Power Converters Under Unstable Conditions



V.Jaya Prakash<sup>1</sup>, K.Kiran Kumar<sup>2</sup>

<sup>1</sup>Student SRKREC, India, v.jp819@gmail.com

<sup>2</sup>Asst.Prof.SRKREC, India, friendlykiran31@gmail.com

**Abstract :** This paper presents a new grid synchronization method for three-phase three-wire networks, namely dual second-order generalized integrator (SOGI) frequency-locked loop. Grid synchronization algorithms are of great importance in the control of grid-connected power converters, as fast and accurate detection of the grid voltage parameters is crucial in order to implement stable control strategies under generic grid conditions. The method is based on two adaptive filters, implemented by using a SOGI on the stationary  $\alpha\beta$  reference frame, and it is able to perform an excellent estimation of the instantaneous symmetrical components of the grid voltage under unbalanced and distorted grid conditions. This paper analyzes the performance of the proposed synchronization method including different design issues. Moreover, the behavior of the method for synchronizing with highly unbalanced grid is proven by means of simulation and experimental results and Hysteresis Current Controller is used as controller of the power converter

**Key words :** Adaptive filters (AFs), electric variables measurements, frequency-locked loops (FLLs), monitoring, power converters, renewable energy, smart grid, synchronization.

## INTRODUCTION

The high penetration of renewable energy sources such as wind power and photo voltaics experienced in the last decades is a good example, as both generation systems are connected to the grid by means of power electronics-based power processors that should not only control the power delivered to the network, but also contribute to the grid stability, supporting the grid services although the various (voltage/frequency) under generic conditions, even under grid faults[3]-[4]. The grid voltage waveforms are sinusoidal and balanced under regular operating conditions, they can easily become unbalanced and distorted due to the effect of grid faults and nonlinear loads. Under these conditions, grid-connected converters should be properly synchronized with the grid in order to stay actively connected, supporting the grid services and keeping the generation up and running. Algorithms based on the implementation of phase-locked loops (PLL) have traditionally been used for synchronizing the control system of power converters with the grid voltage. In Fig. 1, the layout of a generic control structure for a three phase power converter connected to the grid is shown. As depicted in Fig. 1, the grid synchronization block is

responsible for estimating the magnitude frequency and phase angle of the positive- and the negative-sequence components of the grid voltage,  $v_{\pm}$ ,  $\omega$ , and  $\theta_{\pm}$ , respectively. These estimated values are later used at the current controller block, which settles finally the voltage waveform to be modulated  $v_c^*$  as well as at the reference generator, responsible of determining the current reference to be tracked.

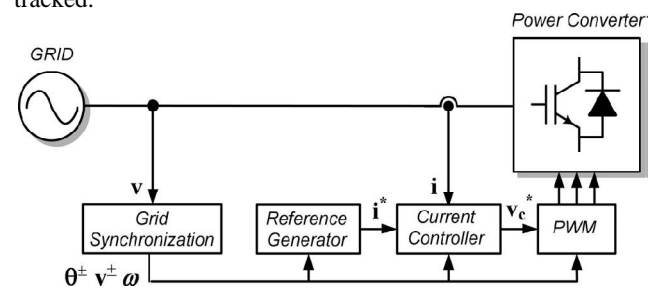


Fig.1

Fig. 1. Generic grid synchronization application for the control of a grid connected three-phase power converter.

In three-phase systems, a PLL based on a synchronous reference frame (SRF-PLL) has become a conventional grid synchronization technique. Nevertheless, the response of the SRF-PLL is unacceptably deficient when the grid voltage is unbalanced due to the appearance of a negative-sequence component that the SRF-PLL is unable to process properly. In order to solve this problem, different advanced grid synchronization systems have recently been proposed. the decoupled double SRF PLL (DDSRFPPLL)[5], an extension of the SRF-PLL, which uses two SRFs and a decoupling network to isolate the effects of the positive and the negative-sequence voltage components

In this paper, a new approach using frequency locking instead of conventional phase locking will be presented as an effective solution for grid synchronization under adverse grid conditions. The proposed synchronization system is based on the basic operation principle presented in [6], on an adaptive filter (AF), implemented by means of a second-order generalized integrator (SOGI), which is self-tuned to the grid frequency thanks to the action of a frequency-locked loop (FLL). Therefore, the proposed synchronization system has been called SOGI-FLL

**SOGI-FLL**

An interesting feature of the GI, when it is used in power converter synchronization applications, is its ability to generate a set of in-quadrature output signals. In the control of grid-connected power converters, these in-quadrature signals are used to estimate the rms value of the grid voltage and current, to calculate the active and reactive power references for the power converter, to generate a leaded/lagged version of the power signal, and to compute the positive- and negative-sequence components in three-phase systems. The two in-quadrature output signals of the AF in Fig. 2 are given by the following transfer functions

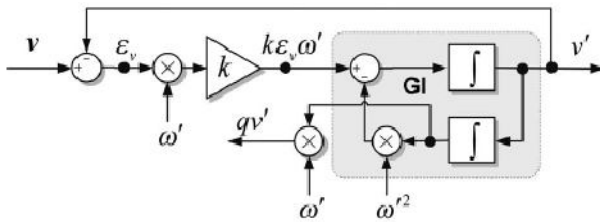


Fig.2 GI with a bandwidth independent of the frequency  $\omega'$  and normalized output amplitude

$$D(s) = \frac{v'}{v}(s) = \frac{k\omega's}{s^2 + k\omega's + \omega'^2} \tag{1}$$

$$Q(s) = \frac{qv'}{v}(s) = \frac{k\omega'^2}{s^2 + k\omega's + \omega'^2} \tag{2}$$

Where

- $\omega'$ —Tuning frequency of the filter
- K— Damping factor of the filter

The Fault location for two terminal networks is carried out by using travelling wave theory with synchronized

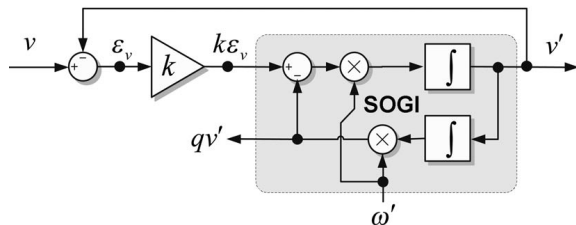


Fig.3 GI with a bandwidth independent of the frequency  $\omega'$  and normalized output amplitude

The AF in Fig. 2 can be considered as a proper solution to synchronize grid-connected power converters, since the bandwidth of the AF depends only on the gain  $k$ , and the amplitude of the in-quadrature signals  $v'$  and  $qv'$  matches the amplitude of the signal  $v$  when the input frequency  $\omega$  is equal to the center frequency of the filter  $\omega'$ . Finally, instead of modifying the structure of the AF, an alternative structure for the GI is proposed in order to achieve the transfer functions written in (4). The new sinusoidal integrator, which is shown in Fig. 3, is called the SOGI. The SOGI transfer function is given by

$$\text{SOGI}(s) = \frac{v'}{k\varepsilon_v}(s) = \frac{\omega's}{s^2 + \omega'^2} \tag{3}$$

The center frequency of the structures in Fig. 3 should be adapted to the frequency of the input signal in order to achieve a balanced set of in-quadrature outputs with the correct amplitudes. In fact, the frequency adaptation mechanisms for these structures share a common philosophy.

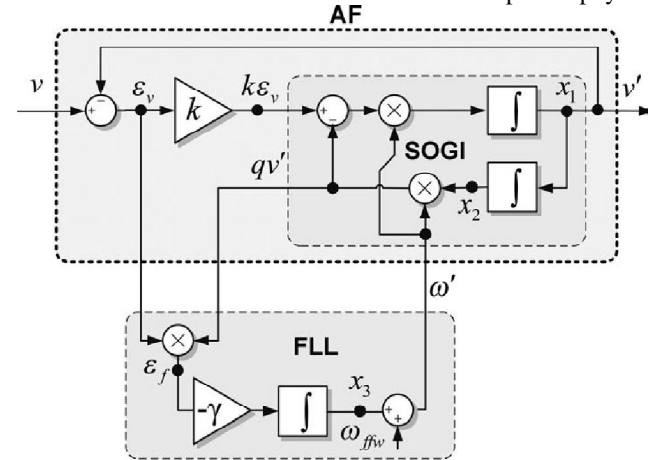


Fig4 : SOGI FLL grid synchronization system

The combination of the SOGI and the FLL building blocks, as shown in Fig. 4 gives rise to a single-phase grid synchronization system known as SOGI-FLL. In the SOGI-FLL, the input frequency is directly detected by the FLL.

**SRF-PLL**

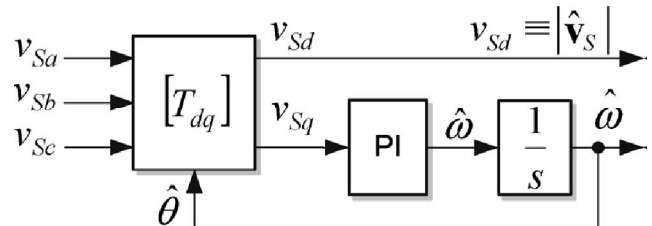


Fig:5 SRF-PLL

In the conventional SRF-PLL, the three-phase voltage vector is translated from the natural reference frame to the rotating reference frame by using Park's transformation as shown in Fig. 5. The angular position of this reference frame is controlled by a feedback loop which regulates the component to zero. Therefore in steady-state, the component depicts

the voltage vector amplitude and its phase is determined by the output of the feedback loop. Under ideal utility conditions, i.e., neither harmonic distortion unbalance, a high band-width of the SRF-PLL feedback loop yields a fast and precise detection of the phase and amplitude of the utility voltage vector. In case the utility voltage is distorted with high-order harmonics, the SRF-PLL can operate satisfactorily if its band width is reduced in order to reject and cancel out the effect of these harmonics on the output. It will be evinced in the following however that the PLL band width reduction is not an acceptable solution in the presence of unbalanced grid voltages. In unbalanced grid operating conditions (without voltage harmonics), the phase voltages with can be generally expressed as

$$v_{S_i} = V_S^{+1} \cos\left(\omega t - k \frac{2\pi}{3}\right) + V_S^{-1} \cos\left(-\omega t - k \frac{2\pi}{3} + \phi^{-1}\right) + V_S^0 \cos(\omega t + \phi^0) \quad [4]$$

where superscripts 1, 1 and 0 define the coefficients for the positive, negative and zero sequence components, and takes values  $k=0, 1, 2$  for  $i=a,b,c$  respectively. Using the non-normalized Clarke transformation, the utility voltage vector is given by

$$v_{S(\alpha\beta\gamma)}^s = \begin{bmatrix} v_{S\alpha} \\ v_{S\beta} \\ v_{S\gamma} \end{bmatrix}^T = [T_{\alpha\beta\gamma}] \begin{bmatrix} v_{S_c} \\ v_{S_b} \\ v_{S_c} \end{bmatrix}$$

$$\text{where } [T_{\alpha\beta\gamma}] = \frac{2}{3} \begin{bmatrix} 1 & -\frac{1}{2} & -\frac{1}{2} \\ 0 & \frac{\sqrt{3}}{2} & -\frac{\sqrt{3}}{2} \\ \frac{1}{2} & \frac{1}{2} & \frac{1}{2} \end{bmatrix}.$$

## DDSRF

The expression of the fundamental voltage vector on the  $\alpha\beta$  reference frame is defined as The superscript +1 and -1 define coefficients of the positive and negative sequence components, respectively. The voltage vector in  $\alpha\beta$  reference frame consists of two sub-vectors:  $V_{s+1}$ , rotating with a positive angular frequency  $\omega$ , and  $V_{s-1}$ , rotating with a negative angular frequency  $-\omega$ . The double SRF is composed of two rotating reference frames:  $dq+1$ , rotating with the positive direction and whose angular positive is  $\Theta'$ , and  $dq-1$ , rotating with the negative direction and whose angular positive is  $-\Theta'$ . The block diagram of DDSRF-PLL is shown in Fig. 2. If the vector in  $\alpha\beta$  reference frame is expressed as

$$v_{s(dq^{+1})} = \begin{bmatrix} v_{sd^{+1}} \\ v_{sq^{+1}} \end{bmatrix} = [T_{dq^{+1}}] v_{s(\alpha\beta)} \quad [6]$$

$$= V_{s+1} \begin{bmatrix} \cos(\alpha\theta - \theta') \\ \sin(\alpha\theta - \theta') \end{bmatrix} + V_{s-1} \begin{bmatrix} \cos(-\alpha\theta + \varphi_{-1} - \theta') \\ \sin(-\alpha\theta + \varphi_{-1} - \theta') \end{bmatrix}$$

$$v_{s(dq^{-1})} = \begin{bmatrix} v_{sd^{-1}} \\ v_{sq^{-1}} \end{bmatrix} = [T_{dq^{-1}}] v_{s(\alpha\beta)} \quad [7]$$

$$= V_{s+1} \begin{bmatrix} \cos(\alpha\theta + \theta') \\ \sin(\alpha\theta + \theta') \end{bmatrix} + V_{s-1} \begin{bmatrix} \cos(-\alpha\theta + \varphi_{-1} + \theta') \\ \sin(-\alpha\theta + \varphi_{-1} + \theta') \end{bmatrix},$$

$$[T_{dq^{+1}}] = [T_{dq^{-1}}] = \begin{bmatrix} \cos(\theta') & \sin(\theta') \\ -\sin(\theta') & \cos(\theta') \end{bmatrix}. \quad [8]$$

The harmonics in source voltages could be restrained by PLL. Based on the small signal analysis,  $\Theta'$  is believed to be equal to the phase  $\omega t$  when the phase is locked. The above Equations should be rewritten as and the  $q$  component should be equal to zero as conventional ones if the oscillation with  $2\omega$  frequency is not included

$$v_{s(dq^{+1})} = V_{s+1} \begin{bmatrix} 1 \\ \alpha\theta - \theta' \end{bmatrix} + V_{s-1} \begin{bmatrix} \cos(-2\alpha\theta + \varphi_{-1}) \\ \sin(-2\alpha\theta + \varphi_{-1}) \end{bmatrix},$$

$$v_{s(dq^{-1})} = V_{s+1} \begin{bmatrix} \cos(2\alpha\theta) \\ \sin(2\alpha\theta) \end{bmatrix} + V_{s-1} \begin{bmatrix} \cos(\varphi_{-1}) \\ \sin(\varphi_{-1}) \end{bmatrix}. \quad [9]$$

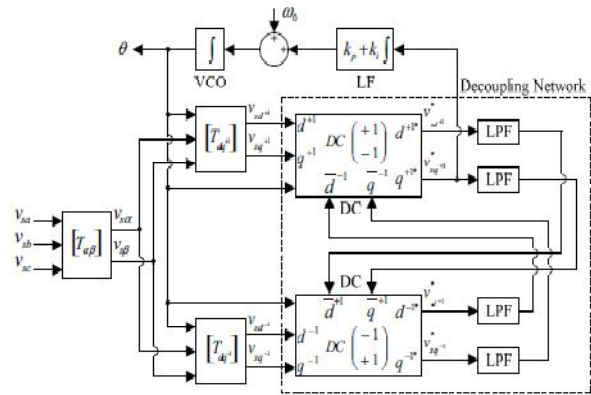


Fig.6 : DDSRF

## TUNING OF THE SOGI-FLL

### A. SOGI Tuning:

sinusoidal input signal  $v = V \sin(\omega t + \phi)$  is written as

$$v' = -\frac{V}{\lambda} \sin(\lambda\omega t) \cdot e^{-(k\omega'/2)t} + V \sin(\omega t)$$

$$qv' = V \left[ \cos(\lambda\omega t) + \frac{k}{2\lambda} \cdot \sin(\lambda\omega t) \right] e^{-(k\omega'/2)t} - V \cos(\omega t) \quad [11]$$

$$\text{where } \lambda = \sqrt{4 - k^2}/2 \text{ and } k < 2. \quad [12]$$

According to the [11][12] equations

$$t_{s(AF)} = \frac{10}{k\omega'}. \quad [13]$$

the higher the value of  $k$ , the faster the response of the SOGI. However, the gain  $k$  affects also the bandwidth of the SOGI, a very high value for  $k$  would reduce the immunity of the SOGI in front of harmonics in the input but, on the other hand, a very low value for  $k$  gives rise to a very long undamped transient response of the SOGI

### B. FLL Tuning:

Linear control analysis techniques cannot directly be applied to determine the value of the FLL gain  $\gamma$ , since the frequency adaptation loop is highly nonlinear. Hence, some assumptions should be made to determine the performance of the FLL.

Considering a sinusoidal signal  $v = V \sin(\omega t + \phi)$  as the input signal for the SOGI and assuming nonstable FLL operating point, with  $\omega' = \omega$ , the square of the state  $x_2$  can be written from

$$\dot{x}_2^2 = \frac{V^2}{2\omega'^2} |D(j\omega)|^2 [1 + \cos(2(\omega t + \phi + \angle D(j\omega)))] \quad [13]$$

The terms  $|D(j\omega)|$  and  $\angle D(j\omega)$  tend toward 1 and 0, respectively, as the frequency detected by the FLL locks the input frequency  $\omega' \rightarrow \omega$ . The averaged dynamics of the FLL with  $\omega_- \approx \omega$  can be described by where the ac component of  $\dot{x}_2^2$  has been neglected

$$\dot{\omega}' = -\frac{\gamma V^2}{k\omega'} (\omega' - \omega)$$

The state equation of is very interesting because it discloses the relationship between the dynamic response of the FLL,

the grid variables, and the SOGI gain the value of  $\gamma$  can be normalized according to

$$\gamma = \frac{k\omega'}{V^2} \Gamma \tag{14}$$

the SOGI and the FLL have been studied by considering separated variations in both the amplitude and the frequency of the input signal. However, both systems are independent, which means that the global time response of the SOGI-FLL will differ from the one obtained whether the input signal experiments simultaneous variations in frequency and amplitude. However, from an analysis based on simulation, it could be considered that the settling times of SOGI and FLL will continue matching to those calculated

if the settle times are in the range of  $t_{s(FLL)} \geq 2 \cdot t_{s(SOGI)}$  for  $k = \sqrt{2}$ , where  $t_{s(FLL)}$  and  $t_{s(SOGI)}$  are the settling times of the FLL and the SOGI, respectively, while  $k$  is the SOGI gain. From now on, a value of  $k = \sqrt{2}$  and  $\Gamma = 50$  will be considered for the following simulations and experiments

**SOGI-FLL APPLIED TO THREE-PHASE SYSTEMS**

Most of the three-phase grid-connected power converters employ a three-wire connection. Therefore, the current injected into the network is exclusively synchronized with the positive- and negative-sequence components of the grid voltage. As a direct consequence, the three-phase voltage vector can be represented in an orthogonal reference frame by means of two independent variables  $\alpha\beta$  thanks to the Clarke transformation. Moreover, taking advantage of Lyon's transformations, the instantaneous positive- and negative-sequence voltage components on the  $\alpha\beta$  reference frame can be calculated as written in

$$\begin{aligned} \mathbf{v}_{\alpha\beta}^+ &= [T_{\alpha\beta}] \mathbf{v}_{abc}^+ - [T_{\alpha\beta}] [T_+] \mathbf{v}_{abc} \\ &= [T_{\alpha\beta}] [T_+] [T_{\alpha\beta}]^T \mathbf{v}_{\alpha\beta} - \frac{1}{2} \begin{bmatrix} 1 & -q \\ q & 1 \end{bmatrix} \mathbf{v}_{\alpha\beta} \end{aligned} \tag{15}$$

$$\begin{aligned} \mathbf{v}_{\alpha\beta}^- &= [T_{\alpha\beta}] \mathbf{v}_{abc}^- = [T_{\alpha\beta}] [T_-] \mathbf{v}_{abc} \\ &= [T_{\alpha\beta}] [T_-] [T_{\alpha\beta}]^T \mathbf{v}_{\alpha\beta} = \frac{1}{2} \begin{bmatrix} 1 & q \\ -q & 1 \end{bmatrix} \mathbf{v}_{\alpha\beta} \end{aligned} \tag{16}$$

where  $q = e^{-j(\pi/2)}$  is a 90° lagging phase-shifting operator applied in the time domain to obtain an in-quadrature version of the input waveforms.

**DSOGI-FLL**

Working in the  $\alpha\beta$  domain, an optimal application of the SOGI-FLL concept for three-phase grid synchronization applications can be found, giving rise to what is known as the DSOGI-FLL, which is graphically presented in Fig. 7. As can be seen, just two SOGIs are necessary to compute the symmetrical components in a three-phase application, one for  $\alpha$  and another for  $\beta$  ( $AF(\alpha), AF(\beta)$ ).

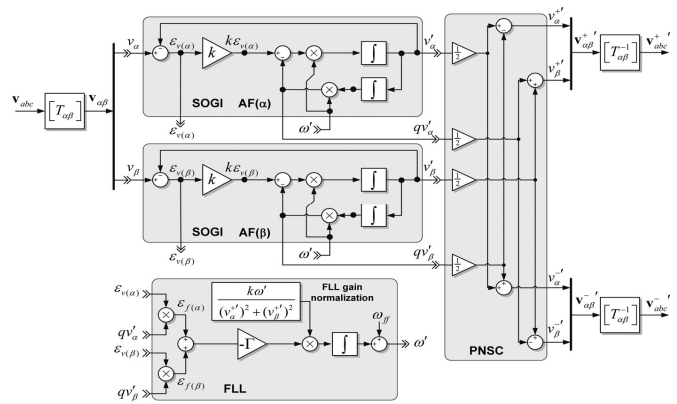


Fig.7: Block diagram of the DSOGI-FLL.

In the DSOGI-FLL in Fig. 7, the two SOGIs are arranged in parallel to provide the input signals to a positive/negative-sequence calculation block (PNSC) the positive sequence of the voltage vector detected by the DSOGI-FLL,

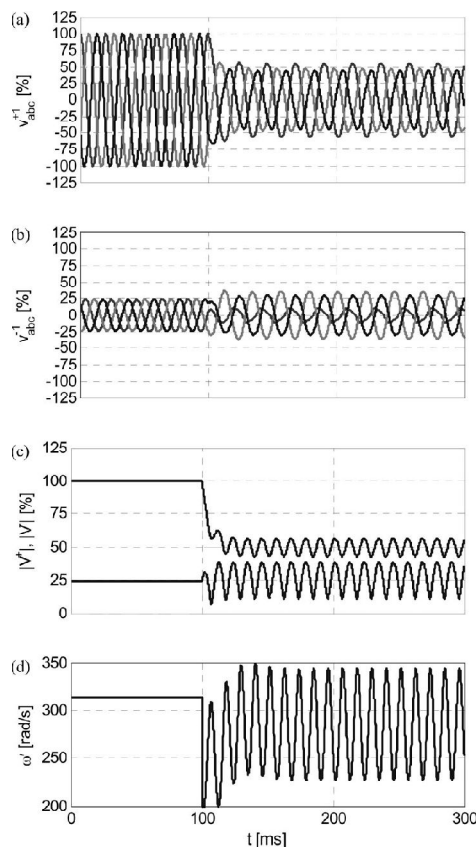


Fig.8: The SRF-PLL(a)-(d) Grid Voltage and frequency variations

## SIMULATION RESULTS

An unbalanced grid voltage sag, affected by jumps in the grid-voltage amplitude, phase angle, and frequency, was applied to its input. the positive- and the negative-sequence voltage phasors of the

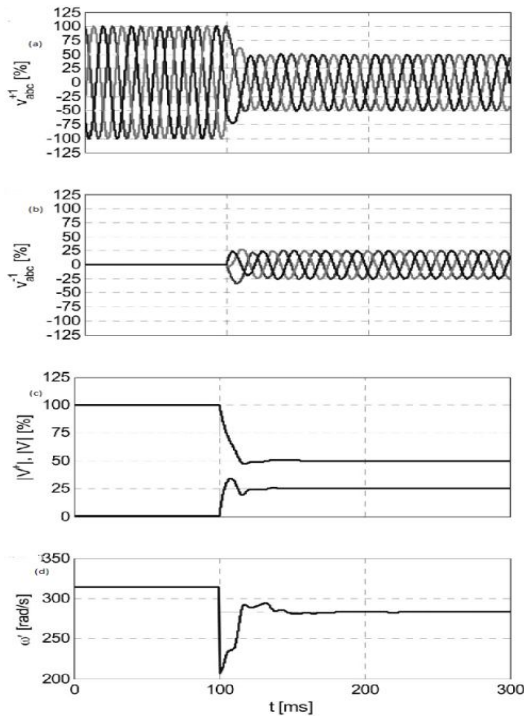


Fig.9: The DDSRF-PLL (a)-(d) with grid voltage and frequency variations

grid voltage were  $\vec{v}^+ = 0.5 \angle -30^\circ$  (P.U.),  $\vec{v}^- = 0.25 \angle 60^\circ$  (P.U), under fault conditions, being the prefault grid voltage equal to  $\vec{v}_{pf=1} = 1 \angle 0^\circ$  (P.U) the input frequency experienced a sudden jump from 50 to 45 Hz as well when the fault occurred. The tuning parameters of the DSOGI-FLL were set to  $k = \sqrt{2}$  and  $\Gamma = 50$ . In Fig. 10(a), the waveforms of the unbalanced grid voltage are depicted. Fig. 10(b) and (c) shows, respectively, the instantaneous positive- and negative-sequence components detected by the DSOGI-FLL. Likewise, the detected grid-voltage amplitude and phase angle for the symmetrical components are drawn in Fig. 10(d)–(f), respectively. All these values have been calculated according to

$$|\vec{v}^\pm| = \sqrt{(v_\alpha^\pm)^2 + (v_\beta^\pm)^2}; \quad \theta^\pm = \tan^{-1} \frac{v_\beta^\pm}{v_\alpha^\pm}$$

.Decoupled double synchronous reference frame Phase-locked loop (DDSRF-PLL) is able to detect the phase angle of positive sequence. To improve the evaluation of the DSOGI-FLL performance, the voltage sag in Fig. 10(a) was also applied to the input of the SRF-PLL and the DDSRF-PLL. In both cases, the tuning of the control parameters has been set in order to achieve the same time constant of the DSOGI-FLL. It can be clearly seen in Fig. 8(a)–(d) that this synchronization method is not robust enough under such unbalanced conditions. As shown in Fig.

9(a) and (b), the estimation of the instantaneous positive and negative-sequence components of the grid voltage is not correct. This is due to the oscillations in both the voltage amplitude and the phase angle estimated by the SRF-PLL under unbalanced conditions as a consequence of the coupling between the positive- and negative-sequence components. When the voltage sag is applied to the DDSRF-PLL the positive- and negative-sequence components estimated by the DDSRF-PLL are close to the ones obtained with the DSOGI-FLL. However, as can be noticed in Fig. 10(d), detection of the grid frequency in the DDSRF-PLL is not as good as the one achieved with the DSOGI-FLL. The DDSRF-PLL is highly influenced by the phase-angle jump of the grid voltage, something that gives rise to a large error in the estimation of such phase angle and, consequently, a large overshoot in the estimated frequency. It can be concluded that the DSOGI-FLL is a very precise and fast synchronization system which is able to detect without any error the instantaneous positive- and negative-sequence components of the faulty grid voltage in about one grid cycle. This performance cannot be achieved by using a classic SRF-PLL and it is even better than the one achieved with a more advanced grid synchronization system, such as the DDSRF-PLL.

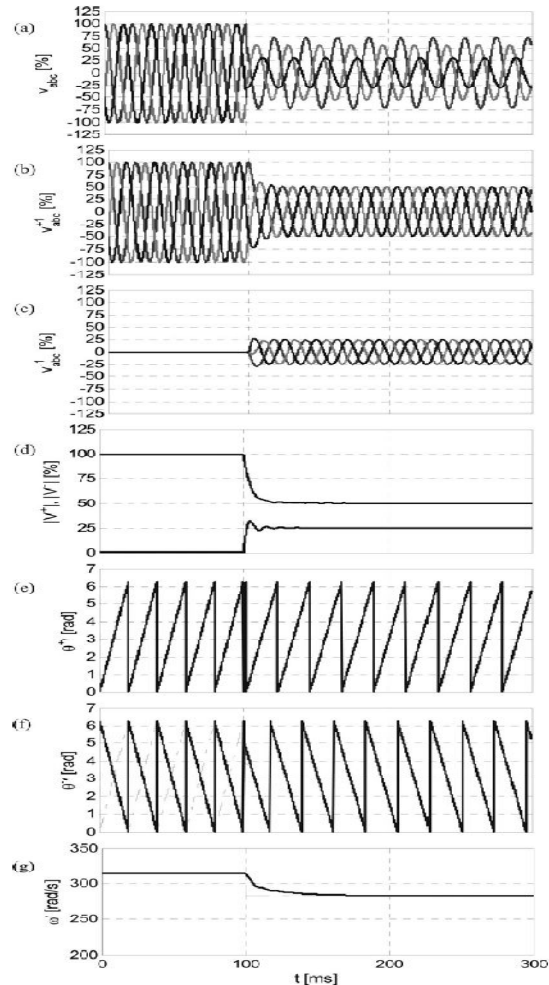


Fig.10: Response of the DSOGI-FLL with voltage amplitude, phase angle, and frequency changes.

## CONCLUSION

A new concept in grid synchronization of power converters under unbalanced and faulty operating conditions, the DSOGIFLL, The DSOGI-FLL consists of three fundamental blocks: 1) the DSOGI, which uses the SOGI as a building block; 2) an FLL that accurately achieves grid-frequency adaptation without involving phase-angle operations; and 3) the PNSC, which implements the instantaneous symmetrical component (ISC) method on the  $\alpha\beta$  reference frame. The proposed synchronization method exploits the ISC method on the stationary and orthogonal  $\alpha\beta$  reference frame, permitting elimination of the zero-sequence component, which cannot be controlled in three-phase three-wire power converters. Moreover, working on the  $\alpha\beta$  reference frame permits reduction of the computational cost of the DSOGI-FLL, since no trigonometric transformations should be performed. As shown in this paper, the presented DSOGI-FLL is a Frequency adaptive system that permits synchronizing to the fundamental-frequency component by means of an FLL instead of a PLL. In this paper, it was shown by simulation that voltage phase-angle detection is not a trivial issue under grid fault conditions. Thus, the DSOGI-FLL is less influenced by sudden changes in the voltage phase angle compared with classical or advanced PLLs. Although a mathematical analysis has demonstrated the nonlinear behavior of the DSOGI-FLL, the application of a feedback-based linearization has permitted us to demonstrate that it is possible to achieve a controllable response of the frequency-adaptation loop as a function of the magnitude and frequency of the input signal. A detailed analysis of the proposed synchronization method has led to expressions that permit setting the tuning parameters in order to achieve a given settle time in the estimation of the amplitude and the frequency.

## REFERENCES.

- [1] Pedro Rodríguez, Alvaro Luna, Raúl Santiago Muñoz-Aguilar, Ion Etxebarria-Otadui, Remus Teodorescu and Frede Blaabjerg, "A Stationary Reference Frame Grid Synchronization System for Three-Phase Grid-Connected Power Converters Under Adverse Grid Conditions" *IEEE Transactions on power electronics*, vol. 27, no. 1, January 2012.
- [2] 2006.F. Iov, A. Hansen, P. Sorensen, and N. Cutululis, "Mapping of grid faults and grid codes," *Risoe Natl. Lab., Tech. Univ. Denmark, Copenhagen, Tech. Rep.*, 2007.
- [3] I. Erlich, W. Winter, and A. Dittrich, "Advanced grid requirements for the integration of wind turbines into the German transmission system," presented at the IEEE Power Engineering Society General Meeting, Duisburg
- [4] University, Germany, 2006 P. Rodriguez, J. Pou, J. Bergas, J. I. Candela, R. P. Burgos, and D. Boroyevich, "Decoupled double synchronous reference frame PLL for power converters control," *IEEE Trans. Power Electron.*, vol. 22, no. 2, pp. 584–592, Mar. 2007.
- [5] P. Rodríguez, A. Luna, I. Candela, R. Mujal, R. Teodorescu, and F. Blaabjerg, "Multiresonant frequency-locked loop for grid synchronization of power converters under distorted grid conditions," *IEEE Trans. Ind. Electron.*, vol. 58, no. 1, pp. 127–138.
- [6] S. Shinnaka, "A Robust single-phase PLL system with stable and fast spacetacking," *IEEE Trans. Ind. Appl.*, vol. 44, no. 2, pp. 624–633, Mar./Apr. 08.
- [7] M. Ciovotaru, V. G. Agelidis, R. Teodorescu, and F. Blaabjerg, "Accurate and less-distributing active antiislanding space method based on PLL for Grid-connected converters," *IEEE Trans. Power Electron.*, vol. 25, no. 6, pp. 1576–1584, Jun. 2010.
- [8] P. Mattavelli, "A closed-loop selective harmonic compensation for active filters," *IEEE Trans. In. Appl.*, vol. 37, no. 1, pp. 81–89, Jan./Feb. 2001
- [9] M. H. J. Bollen, *Understanding Power Quality Problems: Voltage Sags and Interruptions (Power Engineering Series)*. Piscataway, NJ: IEEE Press, 2000.
- [10] X. Yuan, W. Merkh, H. Stemmler, and J. Allmeling, "Stationary frame generalised integrator for current control of active power filter with zero steady-state error for current harmonics of concern under unbalanced and distorted operating conditions," *IEEE Trans. Ind. Electron.*, vol. 56, no. 2, pp. 337–347, Feb. 2009
- [11] F. D. Freijedo, J. Dovel-Gandoy, O. Lopez, and E. Acha, "A Generic open-loop algorithm for three-phase grid voltage/current synchronisation with particular reference to phase, frequency, and amplitude estimation," *IEEE Trans. Power Electron.*, vol. 24, no. 1, pp. 94–107, Jan. 2009